# Electronic structure determination of chromium boride cation, $CrB^+$

Apostolos Kalemos and Aristides Mavridis[a)]
*Laboratory of Physical Chemistry, Department of Chemistry, National and Kapodistrian University of Athens, P.O. Box 64 004, 157 10 Zografou, Athens, Greece*

(Received 23 February 2000; accepted 11 May 2000)

The $CrB^+$ cation molecular system has been investigated with the help of semi-quantitative basis sets $[(7s6p4d3f)_{Cr}/(4s3p2d1f)_B]$ and highly correlated (valence) multi-reference wave functions. Out of a possible manifold of 70 states correlating to the $Cr^+(^6S, ^6D, ^4D, ^4G) + B(^2P)$ atomic states, we have explored a total of 35 states spanning an energy range of about 3.4 eV. The ground state is of $X\,^7\Sigma^+$ symmetry with a binding energy of 28.8 kcal/mol at an internuclear distance of 2.242 Å. The next three excited states $1\,^5\Sigma^+$, $2\,^5\Pi$, and $3\,^7\Pi$ with energy splittings 7.1, 12.9, and 24.3 kcal/mol from the $X$ state, have binding energies of 21.8, 16.5, and 5.1 kcal/mol, respectively. For practically all states we report potential energy curves, total energies, the most common spectroscopic parameters, while we discuss the binding modes using simple chemical diagrams based on valence-bond concepts. © *2000 American Institute of Physics.* [S0021-9606(00)30630-4]

## I. INTRODUCTION

With the present report on $CrB^+$ we conclude our tetralogy on the boride cationic systems $MB^+$, M=Sc, Ti, V, and Cr.[1] As in our previous work in these systems we investigate by *ab initio* quantum mechanical methods, the electronic structure of the ground and of a series of low-lying excited states of the $CrB^+$ molecule. In particular, we focus our attention on the accurate determination of binding energies, and on interpreting the binding modes of the states studied by simple pictures based on a valence-bond conceptual approach.

All states examined correlate to the ground $^2P$ state of the $B$ atom, and to the ground $^6S(3d^5)$ and first three excited states $^6D(4s3d^4)$, $^4D(4s3d^4)$, $^4G(3d^5)$ of the $Cr^+$ cation. The Wigner–Witmer rules dictate that the (adiabatic) interactions $(^6S, ^6D, ^4D, ^4G)_{Cr^+}\otimes{}^2P_B$ give rise to $\{^{5,7}\Sigma^+, ^{5,7}\Pi\}$, $\{^{5,7}\Sigma^+(2), ^{5,7}\Sigma^-, ^{5,7}\Pi(3), ^{5,7}\Delta(2), ^{5,7}\Phi\}$, $\{^{3,5}\Sigma^+(2), ^{3,5}\Sigma^-, ^{3,5}\Pi(3), ^{3,5}\Delta(2), ^{3,5}\Phi\}$, $\{^{3,5}\Sigma^+(2), ^{3,5}\Sigma^-, ^{3,5}\Pi(3), ^{3,5}\Delta(3), ^{3,5}\Phi(3), ^{3,5}\Gamma(2), ^{3,5}H\}$ molecular states spanning an energy range of about 4 eV. Out of the above 70 molecular states we have examined a total of 35, i.e., all of the first (4) and of the second (18) group, all of the triplets (9) of the third group and 4 states $(^3\Sigma^-, ^3\Phi, ^3\Gamma, ^3\Delta)$ of the last group. Due to the rather large $^6D\leftarrow{}^6S$ $Cr^+$ energy splitting (1.522 eV),[2] only the first four states $(X\,^7\Sigma^+, 1\,^5\Sigma^+, 2\,^5\Pi, 3\,^7\Pi)$ are bound with respect to the ground state atoms (*vide infra*).

It is of interest to recall at this point that the ground states of $ScB^+$, $TiB^+$, and $VB^+$ are of high spin symmetry, namely $X\,^4\Sigma^-$, $X\,^5\Delta$, and $X\,^6\Sigma^+$, with $D_e$'s and $R_e$'s of 44.9, 47.6, 42.7 kcal/mol and 2.160, 2.102, and 2.061 Å, respectively,[1] implying similar binding schemes. Indeed, the bonding of the five valence electron $ScB^+$ system in its ground state is succinctly represented by the following valence-bond Lewis (vbL) icon,[1(a)]

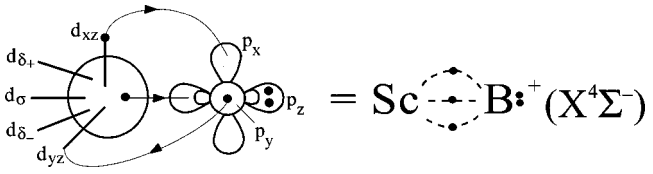


suggesting three half bonds: one $\sigma$ and two $\pi$. The ground states of $TiB^+$ and $VB^+$ are obtained by adding one electron in the $d_{\delta_-}$ (or $d_{\delta_+}$) orbital $(X\,^5\Delta)$, and a second one in the $d_{\delta_+}$ (or $d_{\delta_-}$) orbital $(X\,^6\Sigma^+)$, high spin coupled with the rest $\sigma^1\pi_x^1\pi_y^1$ electrons. The two $d_{\delta_\pm}$ electrons do not participate in the bonding process being completely localized on the metal, something that is rather obvious judging from the similarities of $D_e$'s and $R_e$'s of the three diatomics $ScB^+$, $TiB^+$, and $VB^+$. Similarly, the ground $CrB^+$ state is obtained by grafting an additional electron on the $d_\sigma$ orbital, high spin coupled to the $\sigma^1\pi_x^1\pi_y^1\delta_+^1\delta_-^1$ electron distribution, thus resulting in a $X\,^7\Sigma^+$ state (*vide infra*).

For all 35 states examined in the present work we report potential energy curves (PEC), total energies ($E$), binding energies ($D_e$), spectroscopic parameters, and charge distributions. In Sec. II we outline some technical details, while in Sec. III we touch upon results on the atomic fragments; results and final conclusions are presented in Secs. IV and V.

## II. METHODS

The same basis set was used as in our previous work.[1] For the Cr atom the ANO basis set $20s15p10d6f4g$ of Bauschlicher[3] was used, but without the $g$ functions, generally contracted to $7s6p4d3f$. The triple-$\zeta$ correlation consistent basis, cc-pVTZ, $10s5p2d1f$ of Dunning[4] was employed for the B atom, similarly contracted to $4s3p2d1f$. The resulting one-electron orbital space contains 96 spherical Gaussian functions.

a)Electronic mail: amav@arnold.chem.uoa.gr

 © 2000 American Institute of Physics

Considering the $Cr^+$ $1s^2 2s^2 2p^6 3s^2 3p^6$ and the $B\,1s^2$ electrons as the ''core,'' we are confronted with a 8 ''valence'' (active) electron problem. This $8\,e^-$ system generates $^{2S+1}|\Lambda|$ states with multiplicities 1, 3, 5, 7, and 9. Disregarding the singlet states which correlate to higher excited states of $Cr^+$ than the ones' considered here, and the nonet states which correlate to the first excited $^4P$ state of the B atom, all other multiplicities have been examined. Now with the exception of the septets which, in principle, can be described by a Hartree–Fock wave function, all other states require a multi-reference approach. Moving along the same line as in our previous work,[1] a Complete Active Space SCF (CASSCF) approach was adopted followed by (valence) singles and doubles configuration interaction within the philosophy of the internal contraction.[5] We believe that this multi-reference configuration interaction (MRCI) methodology is the only general method for describing complicated bonded systems,[6,7] particularly if one wishes to construct potential energy curves. We remind that the MRCI method is variational, size consistent and practically size extensive[8,9] for a relatively small number of active electrons.

Our reference space is composed of 10 orbital functions, related asymptotically to the valence occupied spaces of $Cr^+$ $(4s+3d)$ and B $(2s+2p)$ atoms. The number of configuration functions (CF) ensuing from distributing eight electrons among a 10 orbital function space ranges from 268 ($^7\Sigma^-$) to 5200 ($^3\Pi$), according to the symmetry of the state. Our largest MRCI expansion of 15 623 942 CFs is reduced to 815 020 CFs through the internal contraction technique.[5] No significant hazard is caused by the internal contraction strategy; as we are taught from our previous experience[1(b)] total energy losses are of the order of 1 mhartree.

Notwithstanding the $C_{2v}$ symmetry constraints imposed on our computations, the CASSCF wave functions display symmetry and equivalency restrictions. Except otherwise stated all states have been calculated using the state-average technique.[10] Judging as adequate the size of the one particle function space no corrections for basis set superposition errors were applied.

All calculations were done with the MOLPRO 96.4 suite of codes.[11]

## III. THE $Cr^+$ AND B FRAGMENTS

In Table I we report total energies of the $Cr^+$ $^6S(3d^5)$, $^6D(4s3d^4)$, $^4D(4s3d^4)$, $^4G(3d^5)$, and of the B atom $^2P(2s^2 2p)$ and $^4P(2s2p^2)$ spectroscopic terms in different methodologies, as well as corresponding energy splittings. For reasons of completeness calculations on the Cr $^7S(4s3d^5)$, $^5S(4s3d^5)$, and $^5D(4s^2 3d^4)$ states are also reported along with their energy gaps. With the exception of the $Cr^+$ $^4G \leftarrow {}^4D$ energy splitting the rest of the energy gaps are in fair harmony with the experimental values.[2]

## IV. RESULTS AND DISCUSSION

In the following discussion we examine the 35 computed states in ascending energy order and according to their asymptotic products. Figure 1 presents full potential energy curves (PEC) of all states examined and Fig. 2 the corresponding energy level diagram. The ground state is marked with $X$ while the rest of the states have been tagged with numbers in accord with their energy position, i.e., ''1'' for the first, ''34'' for the highest state, 77 kcal/mol above the $X$-state. Table II summarizes our numerical findings, namely, absolute energies ($E$), bond lengths ($R_e$), dissociation energies ($D_e$), harmonic frequencies ($\omega_e$), and energy gaps ($T_e$) of the 35 examined states at the CASSCF, MRCI, and MRCI+$Q$ (MRCI+multireference Davidson correction for unlinked clusters[14]).

### A. The $X\,^7\Sigma^+$, $1\,^5\Sigma^+$, $2\,^5\Pi$, and $3\,^7\Pi$ states

The PECs (at the MRCI level) of the titled states are shown in Fig. 3 correlating to $Cr^+(^6S)+B(^2P)$.

#### 1. $X\,^7\Sigma^+$

As was already mentioned in the Introduction, the ground state of the $CrB^+$ molecule is obtained by distributing three electrons to the remaining $d$-like holes of the $ScB^+$ ($X\,^4\Sigma^-$) system, all of them high spin coupled. Due to the maximal spin this state is adequately described within the Hartree–Fock ansatz. Indeed, the leading CAS equilibrium configuration (HF) is

$$|X\,^7\Sigma^+\rangle \sim 0.97|1\sigma^2 2\sigma^1 3\sigma^1 1\delta_+^1 1\pi_x^1 1\pi_y^1 1\delta_-^1\rangle,$$

with the $1\sigma$ being practically the $2s$ boron atomic orbital. At infinity the $X\,^7\Sigma^+$ state is described by the product wave function $|Cr^+(3d^5),\,^6S\rangle \otimes |B(2s^2 2p),\,^2P; M=0\rangle$.

To investigate the consistency of our calculations different approaches were tried for the titled four states, ranging from (single reference) CISD to MRCI including the ''core'' $3s^2 3p^6$ $Cr^+$ $e^-$ ($c$-MRCI), and increasing also the basis set of boron from triple- to quadruple-$\zeta$. The results are similar for all four states; a representative sample of these calculations is given in Table III for the $X\,^7\Sigma^+$ state. We conclude that the 10 active orbital space (8/10) is necessary even for these states where the $4s$ function of $Cr^+$ is not required asymptotically, the resulting gain in $D_e$ being 1.8 kcal/mol. Going from MRCI to $c$-MRCI the binding is increased by another 1.3 kcal/mol, despite the fact that the ANO-Cr basis set used is not tuned for the $3s^2 3p^6\,e^-$ to be included in the CI treatment.[3] However, we choose not to pursue this point any further due to the disproportional increase of the calculation (92 265 CFs at the MRCI vs 3 849 489 CFs at the $c$-MRCI for the $X\,^7\Sigma^+$ state). Finally, the gain in $D_e$ is rather insignificant, 0.3 kcal/mol by increasing the boron basis from triple- to quadruple-$\zeta$.

An observation is needed at this point for the state average (sa-MRCI) $D_e$ number: the 2.5 kcal/mol $D_e$ difference between the sa-MRCI and MRCI (Table III), is an artifact due to the inappropriateness of the sa-orbitals at infinity as evidenced by the size extensivity error, 7.6 mhartree at the sa-MRCI level. This is not observed to the rest 31 molecular states correlating to the excited $Cr^+$ atomic states. The foregoing discussion justifies our basis set active space (8/10) and MRCI choices.

Now at equilibrium the atomic CASSCF Mulliken populations are (Cr/B)

TABLE I. Total energies (hartree) of the Cr $^7S(4s3d^5)$, $^5S(4s3d^5)$, and $^5D(4s^23d^4)$ states, of the $Cr^+$ $^6S(3d^5)$, $^6D(4s3d^4)$, $^4D(4s3d^4)$, and $^4G(3d^5)$ states, of the B $^2P(2s^22p)$ and $^4P(2s2p^2)$ states, and corresponding energy splittings (eV) in different methodologies.

| | Cr | | | | |
|---|---|---|---|---|---|
| Method | $^7S$ | $^5S$ | $^5D$ | $^5S\leftarrow{}^7S$ | $^5D\leftarrow{}^5S$ |
| NHF[a] | −1043.356 38 | | −1043.309 82 | | |
| SA-SCF[b] | −1043.355 90 | −1043.316 61 | −1043.309 39 | 1.069 | 0.197 |
| CISD($6e^-$) | −1043.455 60 | −1043.420 80 | −1043.411 23 | 0.947 | 0.260 |
| CISD($14e^-$)[c] | −1043.742 95 | −1043.703 19 | −1043.693 85 | 1.082 | 0.254 |
| SA-CASSCF[b] | | | −1043.342 77 | | |
| MRCI($6e^-$) | | | −1043.417 03 | | 0.103 |
| Expt.[d] | | | | 0.941 | 0.062 |

| | $Cr^+$ | | | |
|---|---|---|---|---|
| Method | $^6S$ | $^6D$ | $^4D$ | $^4G$ |
| NHF[e] | −1043.139 39 | | | |
| SA-SCF[b] | −1043.138 83 | −1043.096 49 | −1043.056 01 | −1043.018 90 |
| CISD($5e^-$) | −1043.220 89 | −1043.157 42 | −1043.124 28 | −1043.111 52 |
| CISD($13e^-$)[c] | −1043.506 48 | −1043.450 22 | −1043.411 99 | - |

| | $Cr^+$ energy splittings | | |
|---|---|---|---|
| Method | $^6D\leftarrow{}^6S$ | $^4D\leftarrow{}^6D$ | $^4G\leftarrow{}^4D$ |
| SA-SCF[b] | 1.152 | 1.102 | 1.010 |
| CISD | 1.727 | 0.902 | 0.347 |
| CISD[c] | 1.531 | 1.040 | - |
| Expt.[d] | 1.522 | 0.936 | 0.085 |

| | B | | |
|---|---|---|---|
| Method | $^2P$ | $^4P$ | $^4P\leftarrow{}^2P$ |
| NHF[a] | −24.529 06 | | |
| SCF | −24.528 15 | −24.451 29 | 2.091 |
| CISD | −24.596 63 | −24.467 24 | 3.521 |
| SA-SCF[b] | −24.528 10 | −24.449 31 | 2.144 |
| CISD | −24.596 55 | −24.467 21 | 3.520 |
| SA-CASSCF[b] | −24.559 33 | | |
| MRCI | −24.598 40 | | 3.570 |
| Expt.[d] | | | 3.571 |

[a]Numerical Hartree–Fock, Ref. 12.
[b]Spherically averaged SCF or CASSCF.
[c]The $3s^23p^6$ ''core'' electrons have been added in the CI treatment.
[d]Experimental values, Ref. 2.
[e]Reference 13.

$$4s^{0.36}4p_z^{0.10}3d_{z^2}^{0.95}3d_{xz}^{0.95}3d_{yz}^{0.95}3d_{x^2-y^2}^{1.0}3d_{xy}^{1.0}/$$
$$2s^{1.73}2p_z^{0.79}2p_x^{0.08}2p_y^{0.08},$$

suggesting the following valence-bond Lewis (vbL) bonding picture:

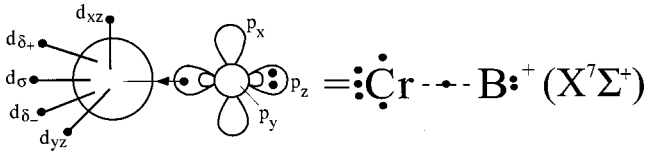


The diagram indicates that the two atoms are held by a half $\sigma$-bond, with five nonparticipating, strictly localized on the metal (observer), electrons; about $0.3\,e^-$ are transferred from B to $Cr^+$ via the $\sigma$-frame. The complete localization of the

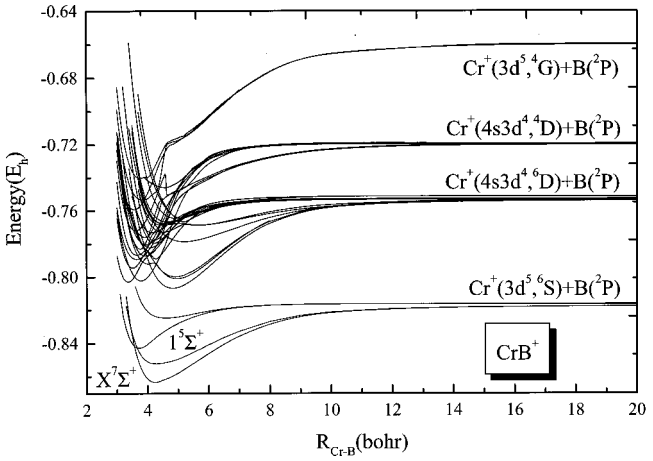


FIG. 1. Potential energy curves of the $CrB^+$ molecule of all 35 states studied at the MRCI level of theory.

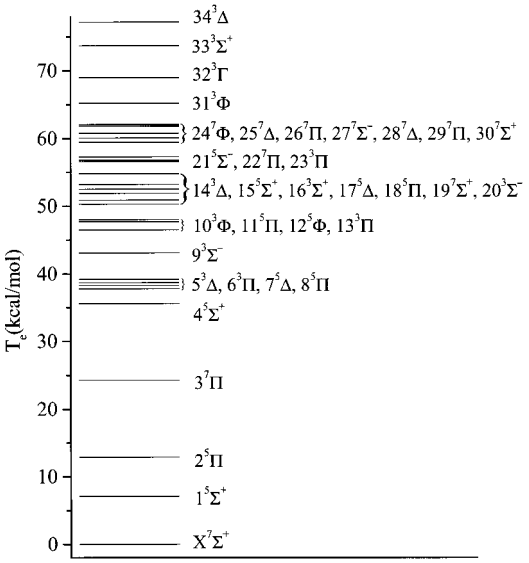


FIG. 2. Relative energy splittings ($T_e$) of all computed states at the MRCI level.

$d_\pi$ electrons as compared to the $ScB^+$, $TiB^+$, and $VB^+$ species,[1] can be rationalized by realizing that the ionization potential (I.P.) of the $Cr^+$ cation is 3.6, 2.9, and 2.3 eV higher than the I.P. of $Sc^+$, $Ti^+$, and $V^+$, respectively.[2] As a result the $D_e$ of $CrB^+$ is abruptly reduced to 29 kcal/mol (MRCI) from a mean value of 45 kcal/mol in the earlier borides,[1] with a concomitant bond length increase ranging from 0.08 ($ScB^+$) to 0.14 ($TiB^+$) to 0.18 ($VB^+$) Å.

#### 2. $1\,^5\Sigma^+$

By a single spin flipping of the $X\,^7\Sigma^+$ the $1\,^5\Sigma^+$ state obtains. Conceptually, we can think that the B atom approaches from infinity to the $Cr^+\ ^6S$ ($M_s=+5/2$) state, with its $p_\sigma$ spin in a $\beta$-like fashion. The bonding is captured by the same vbL icon given previously for the ground state, in agreement with the following dominant CASSCF equilibrium configurations and Mulliken population distributions:

$$|1\,^5\Sigma^+\rangle \sim -0.67|1\sigma^2 2\sigma^2 1\delta_+^1 1\pi_x^1 1\pi_y^1 1\delta_-^1\rangle + 0.43|1\sigma^2 1\delta_+^1 3\sigma^2 1\pi_x^1 1\pi_y^1 1\delta_-^1\rangle + 0.32|1\sigma^2 2\sigma^1 1\delta_+^1 3\bar{\sigma}^1 1\pi_x^1 1\pi_y^1 1\delta_-^1\rangle + 0.31|1\sigma^2 2\bar{\sigma}^1 1\delta_+^1 3\sigma^1 1\pi_x^1 1\pi_y^1 1\delta_-^1\rangle,$$

$$4s^{0.13}4p_z^{0.09}3d_{z^2}^{1.03}3d_{xz}^{0.97}3d_{yz}^{0.97}3d_{x^2-y^2}^{1.0}3d_{xy}^{1.0}/\ 2s^{1.72}2p_z^{0.95}2p_x^{0.06}2p_y^{0.06}.$$

From the B atom $0.2\,e^-$ are transferred to the $Cr^+$ atom via the $\sigma$-frame. At the equilibrium distance of 2.260 Å the binding energy is $D_e=21.8$ kcal/mol, 7.1 kcal/mol less than the binding energy of the $X\,^7\Sigma^+$ state due to the spin flip.

#### 3. $2\,^5\Pi$, $3\,^7\Pi$

The potential curves are shown in Fig. 3 with asymptotic wave functions whose symmetry is carried by the $p_\pi e^-$ of the B atom. The dominant equilibrium CASSCF ($B_1$ symmetry) configurations,

$$|2\,^5\Pi\rangle \sim -0.79|1\sigma^2 1\delta_+^1 2\sigma^1 1\pi_x^2 1\pi_y^1 1\delta_-^1\rangle + 0.24|1\sigma^2 1\delta_+^1 2\sigma^1 2\pi_x^2 1\pi_y^1 1\delta_-^1\rangle + 0.50|1\sigma^2 1\delta_+^1 2\sigma^1 1\pi_x^1 2\bar{\pi}_x^1 1\pi_y^1 1\delta_-^1\rangle,$$

in conjunction with the Mulliken distribution,

$$4s^{0.17}4p_z^{0.11}3d_{z^2}^{0.88}3d_{xz}^{1.0}3d_{yz}^{1.0}3d_{x^2-y^2}^{1.0}3d_{xy}^{1.0}/\ 2s^{1.54}2p_z^{0.25}2p_x^{1.0}2p_y^{0.06},$$

imply the following bonding picture:

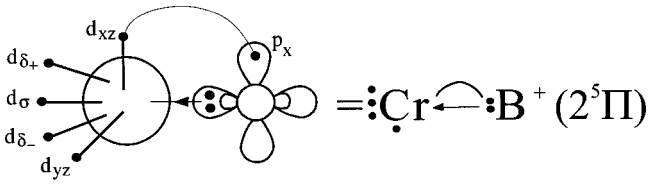


The two atoms are kept together by a $\pi$-bond and a dative $\sigma$-bond originating from the B atom; the character of the double bond is reflected to the rather short bond length, $R_e=1.970$ Å at the MRCI level, despite the low $D_e$ of 16.5 kcal/mol (Table II). Notice that no electrons are transferred through the $\pi$ system, with $0.18\,e^-$ migrating from B to $Cr^+$ via the $\sigma$-frame.

In the next $3\,^7\Pi$ state, the six ''parallel'' electrons *a priori* preclude any real bonding, and indeed a $D_e$ of 5.1 kcal/mol is computed at $R_e=2.435$ Å with a total charge transfer from B to $Cr^+$ of a mere $0.1\,e^-$.

### B. In what follows next we discuss all molecular states stemming from $Cr^+(4s3d^4;{}^6D)+B({}^2P)$, i.e., $4\,^5\Sigma^+$, $7\,^5\Delta$, $8\,^5\Pi$, $11\,^5\Pi$, $12\,^5\Phi$, $15\,^5\Sigma^+$, $17\,^5\Delta$, $18\,^5\Pi$, $19\,^7\Sigma^+$, $21\,^5\Sigma^-$, $22\,^7\Pi$, $24\,^7\Phi$, $25\,^7\Delta$, $26\,^7\Pi$, $27\,^7\Sigma^-$, $28\,^7\Delta$, $29\,^7\Pi$, and $30\,^7\Sigma^+$

#### 1. $4\,^5\Sigma^+$, $15\,^5\Sigma^+$

The PECs of both states are shown in Fig. 4 correlating to $Cr^+({}^6D;M=0,\pm1)+B({}^2P;M=0,\mp1)$. The leading CASSCF equilibrium configurations and corresponding Mulliken populations are

$$|4\,^5\Sigma^+\rangle \sim 0.83|1\sigma^2 2\sigma^2 1\delta_+^1 1\pi_x^1 1\pi_y^1 1\delta_-^1\rangle,$$

$$|15\,^5\Sigma^+\rangle \sim 0.53|1\sigma^2 2\sigma^1 1\delta_+^1 3\bar{\sigma}^1 1\pi_x^1 1\pi_y^1 1\delta_-^1\rangle - 0.40|1\sigma^2 2\sigma^1 1\delta_+^1 3\sigma^1(1\pi_x^1 1\bar{\pi}_y^1 + 1\bar{\pi}_x^1 1\pi_y^1)1\delta_-^1\rangle + 0.26|1\sigma^2 2\sigma^1 1\delta_+^1 3\sigma^1(1\pi_x^1 2\bar{\pi}_y^1 + 2\bar{\pi}_x^1 1\pi_y^1)1\delta_-^1\rangle,$$

$$4\,^5\Sigma^+: 4s^{1.06}4p_z^{0.07}3d_{z^2}^{0.10}3d_{xz}^{1.0}3d_{yz}^{1.0}3d_{x^2-y^2}^{1.0}3d_{xy}^{1.0}/\ 2s^{1.80}2p_z^{0.83}2p_x^{0.05}2p_y^{0.05},$$

$$15\,^5\Sigma^+: 4s^{0.79}4p_z^{0.09}3d_{z^2}^{0.88}3d_{xz}^{0.75}3d_{yz}^{0.75}3d_{x^2-y^2}^{1.0}3d_{xy}^{1.0}/\ 2s^{1.60}2p_z^{0.59}2p_x^{0.26}2p_y^{0.26}.$$

TABLE II. Total energies $E$ (hartree), bond distances $R_e$ (Å), dissociation energies $D_e$ (kcal/mol), harmonic frequencies $\omega_e$ ($cm^{-1}$), and energy gaps $T_e$ (kcal/mol) of the $CrB^+$ states studied in ascending energy order.

| State[a] | Method[b,c] | $-E$ | $R_e$ | $D_e$[d] | $\omega_e$ | $T_e$ | State[a] | Method[b,c] | $-E$ | $R_e$ | $D_e$[d] | $\omega_e$ | $T_e$ |
|---|---|---|---|---|---|---|---|---|---|---|---|---|---|
| $X\ ^7\Sigma^+$ | CASSCF | 1067.740 67 | 2.606 | 18.8 | 257 | | $18\ ^5\Pi$ | MRCI | 1067.778 72 | 2.224 | 16.2 | 675 | 53.2 |
| | MRCI | 1067.863 45 | 2.242 | 28.8 | 436 | 0.0 | | MRCI+Q | 1067.786 2 | 2.225 | 18.1 | 655 | |
| | MRCI+Q | 1067.870 5 | 2.229 | 30.6 | 462 | | $19\ ^7\Sigma^+$ | CASSCF | 1067.664 61 | 3.124 | 8.4 | 125 | |
| $1\ ^5\Sigma^+$ | CASSCF | 1067.732 75 | 2.702 | 13.8 | 173 | | | MRCI | 1067.778 64 | 2.757 | 16.2 | 195 | 53.2 |
| | MRCI | 1067.852 16 | 2.260 | 21.8 | 239 | 7.1 | | MRCI+Q | 1067.785 7 | 2.734 | 17.7 | 199 | |
| | MRCI+Q | 1067.859 1 | 2.242 | 23.5 | 248 | | $20\ ^3\Sigma^-$ | CASSCF | 1067.641 96 | 2.048 | 54.6 | 788 | |
| $2\ ^5\Pi$ | CASSCF | 1067.709 11 | 2.060 | 3.8 | 203 | | | MRCI | 1067.776 18 | 2.075 | 73.0 | 559 | 54.8 |
| | MRCI | 1067.842 84 | 1.970 | 16.5 | 494 | 12.9 | | MRCI+Q | 1067.784 8 | 2.111 | 74.5 | 526 | |
| | MRCI+Q | 1067.850 5 | 1.970 | 18.1 | 507 | | $21\ ^5\Sigma^-$ | MRCI | 1067.773 21 | 2.203 | 12.3 | 434 | 56.6 |
| $3\ ^7\Pi$ | CASSCF | 1067.705 82 | 2.893 | 1.8 | 115 | | | MRCI+Q | 1067.781 6 | 2.195 | 14.8 | 452 | |
| | MRCI | 1067.824 73 | 2.435 | 5.1 | 182 | 24.3 | $22\ ^7\Pi(g)$ | CASSCF | 1067.661 52 | 3.075 | 6.8 | 161 | |
| | MRCI+Q | 1067.831 2 | 2.367 | 6.0 | 202 | | | MRCI | 1067.772 97 | 2.381 | 13.0 | 352 | 56.8 |
| $4\ ^5\Sigma^+$ | CASSCF | 1067.690 29 | 2.677 | 24.5 | 284 | | | MRCI+Q | 1067.781 0 | 2.359 | 15.0 | 374 | |
| | MRCI | 1067.806 77 | 2.551 | 33.8 | 315 | 35.6 | $22\ ^7\Pi(l)$ | MRCI | 1067.768 78 | 2.993 | 10.4 | 164 | |
| | MRCI+Q | 1067.813 6 | 2.540 | 35.3 | 315 | | | MRCI+Q | 1067.775 0 | 2.979 | 11.2 | 176 | |
| $5\ ^3\Delta$ | CASSCF | 1067.668 19 | 1.779 | 33.6 | 747 | | $23\ ^3\Pi$ | CASSCF | 1067.633 05 | 1.920 | 11.0 | 637 | |
| | MRCI | 1067.803 18 | 1.779 | 52.9 | 725 | 37.8 | | MRCI | 1067.772 20 | 1.911 | 33.0 | 631 | 57.3 |
| | MRCI+Q | 1067.810 8 | 1.784 | 54.2 | 715 | | | MRCI+Q | 1067.781 2 | 1.917 | 35.1 | 620 | |
| $6\ ^3\Pi$ | CASSCF | 1067.669 39 | 2.041 | 34.6 | 499 | | $24\ ^7\Phi$ | CASSCF | 1067.655 22 | 2.770 | 1.2 | 120 | |
| | MRCI | 1067.802 42 | 2.003 | 52.3 | 547 | 38.3 | | MRCI | 1067.768 72 | 2.367 | 9.9 | 312 | 59.4 |
| | MRCI+Q | 1067.810 8 | 2.006 | 53.9 | 551 | | | MRCI+Q | 1067.777 1 | 2.338 | 12.4 | 344 | |
| $7\ ^5\Delta$ | CASSCF | 1067.694 51 | 2.755 | 21.3 | 256 | | $25\ ^7\Delta(g)$ | CASSCF | 1067.666 91 | 3.234 | 6.6 | 120 | |
| | MRCI | 1067.801 75 | 2.611 | 29.3 | 285 | 38.7 | | MRCI | 1067.768 69 | 3.015 | 9.5 | 156 | 59.5 |
| | MRCI+Q | 1067.807 6 | 2.595 | 30.6 | 288 | | | MRCI+Q | 1067.773 9 | 2.974 | 10.1 | 137 | |
| $8\ ^5\Pi(g)$ | CASSCF | 1067.687 08 | 2.720 | 22.9 | 287 | | $25\ ^7\Delta(l)$ | MRCI | 1067.768 34 | 2.440 | 9.3 | 277 | |
| | MRCI | 1067.801 00 | 2.623 | 30.6 | 297 | 39.2 | | MRCI+Q | 1067.776 3 | 2.401 | 11.6 | 325 | |
| | MRCI+Q | 1067.807 8 | 2.616 | 31.8 | 307 | | $26\ ^7\Pi(g)$ | MRCI | 1067.767 67 | 2.393 | 9.3 | 302 | 60.1 |
| $8\ ^5\Pi(l)$ | MRCI | 1067.792 14 | 2.126 | 25.0 | 445 | | | MRCI+Q | 1067.775 6 | 2.363 | 11.6 | 327 | |
| | MRCI+Q | 1067.801 4 | 2.122 | 27.8 | 498 | | $26\ ^7\Pi(l)$ | CASSCF | 1067.657 74 | 2.75 | 2.7 | | |
| $9\ ^3\Sigma^-$ | CASSCF | 1067.654 05 | 1.869 | 24.3 | 777 | | | MRCI | 1067.766 79 | 2.75 | 8.8 | | |
| | MRCI | 1067.794 79 | 1.864 | 47.3 | 675 | 43.1 | | MRCI+Q | 1067.773 2 | 2.75 | 10.0 | | |
| | MRCI+Q | 1067.803 8 | 1.869 | 49.5 | 664 | | $27\ ^7\Sigma^-$ | CASSCF | 1067.656 81 | 2.901 | 0.7 | 110 | |
| $10\ ^3\Phi$ | CASSCF | 1067.658 04 | 1.924 | 26.4 | 492 | | | MRCI | 1067.766 56 | 2.453 | 8.2 | 282 | 60.8 |
| | MRCI | 1067.789 38 | 1.923 | 43.6 | 501 | 46.5 | | MRCI+Q | 1067.774 3 | 2.418 | 10.2 | 313 | |
| | MRCI+Q | 1067.797 0 | 1.936 | 44.9 | 488 | | $28\ ^7\Delta$ | CASSCF | 1067.657 23 | 2.863 | 1.0 | 120 | |
| $11\ ^5\Pi$ | CASSCF | 1067.660 3 | ~2.3 | 4.4 | | | | MRCI | 1067.764 92 | 2.710 | 7.1 | 340 | 61.8 |
| | MRCI | 1067.789 31 | ~2.3 | 22.9 | | 46.5 | | MRCI+Q | 1067.770 8 | 2.716 | 8.0 | 357 | |
| | MRCI+Q | 1067.798 4 | ~2.3 | 25.9 | | | $29\ ^7\Pi$ | CASSCF | 1067.654 86 | 2.827 | 0.9 | 113 | |
| $12\ ^5\Phi$ | CASSCF | 1067.658 29 | 2.129 | 3.1 | 383 | | | MRCI | 1067.764 60 | 2.65 | 7.3 | | 62.0 |
| | MRCI | 1067.787 36 | 2.079 | 21.6 | 501 | 47.7 | | MRCI+Q | 1067.771 2 | 2.65 | 8.7 | | |
| | MRCI+Q | 1067.795 7 | 2.085 | 24.1 | 501 | | $30\ ^7\Sigma^+$ | CASSCF | 1067.645 97 | 2.977 | 0.6 | 122 | |
| $13\ ^3\Pi$ | CASSCF | 1067.653 65 | 1.968 | 23.6 | 515 | | | MRCI | 1067.764 55 | 2.613 | 8.2 | 256 | 62.1 |
| | MRCI | 1067.786 89 | 1.931 | 42.1 | 560 | 48.0 | | MRCI+Q | 1067.773 6 | 2.573 | 13.9 | 279 | |
| | MRCI+Q | 1067.794 9 | 1.934 | 43.6 | 547 | | $31\ ^3\Phi$ | CASSCF | 1067.618 97 | 1.877 | 40.2 | 691 | |
| $14\ ^3\Delta$ | CASSCF | 1067.649 62 | 1.980 | 21.5 | 880 | | | MRCI | 1067.759 53 | 1.888 | 62.5 | 646 | 65.2 |
| | MRCI | 1067.783 36 | 1.985 | 39.9 | 792 | 50.3 | | MRCI+Q | 1067.769 3 | 1.898 | 64.8 | 624 | |
| | MRCI+Q | 1067.791 5 | 1.988 | 41.6 | 782 | | $32\ ^3\Gamma$ | CASSCF | 1067.609 32 | 1.955 | 33.6 | 595 | |
| $15\ ^5\Sigma^+$ | CASSCF | 1067.647 58 | 2.243 | 1.7 | 268 | | | MRCI | 1067.753 43 | 2.020 | 58.7 | 456 | 69.0 |
| | MRCI | 1067.782 34 | 2.163 | 19.4 | 456 | 50.9 | | MRCI+Q | 1067.765 2 | 2.072 | 62.4 | 377 | |
| | MRCI+Q | 1067.792 0 | 2.167 | 22.0 | 402 | | $33\ ^3\Sigma^+$ | CASSCF | 1067.626 31 | 2.580 | 6.8 | 397 | |
| $16\ ^3\Sigma^+$ | CASSCF | 1067.646 61 | 2.131 | 19.0 | 463 | | | MRCI | 1067.745 96 | 2.423 | 16.5 | 355 | 73.7 |
| | MRCI | 1067.780 77 | 2.090 | 38.0 | 501 | 51.9 | $34\ ^3\Delta$ | CASSCF | 1067.601 79 | 2.002 | 29.4 | 577 | |
| | MRCI+Q | 1067.789 7 | 2.096 | 40.3 | 511 | | | MRCI | 1067.740 39 | 1.986 | 50.5 | 474 | 77.2 |
| $17\ ^5\Delta$ | MRCI | 1067.779 80 | 2.231 | 16.5 | 588 | 52.5 | | MRCI+Q | 1067.750 8 | 1.976 | 53.2 | 561 | |
| | MRCI+Q | 1067.788 3 | 2.235 | 19.0 | 603 | | | | | | | | |

[a]"$g$" and "$l$" refer to global and local minima.
[b]With the exception of $X\ ^7\Sigma^+$, $1\ ^5\Sigma^+$, $2\ ^5\Pi$, $3\ ^7\Pi$, and $7\ ^5\Delta$, all other states have been computed by the state average technique.
[c]$+Q$ refers to the multi-reference Davidson correction, Ref. 14.
[d]Dissociation energies with respect to the adiabatic fragments.

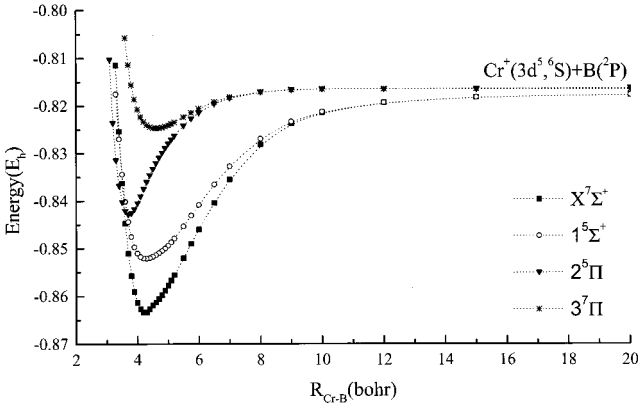


FIG. 3. MRCI PECs of all possible states correlating to $Cr^+(^6S)+B(^2P)$.

Clearly, for the $4\,^5\Sigma^+$ state $4\,e^-$ are completely localized to the $d_\pi$ and $d_\delta$ orbitals; 0.15 and $0.10\,e^-$ are transferred from the $2p_z$ and $2s$ functions of the B atom to a hybrid $(4s4p_z3d_{z^2})^{1.23}$ orbital of the $Cr^+$ cation creating a $\sigma$-bond $(\sim 2\sigma^2)$. The bonding is captured by the following vbL icon:

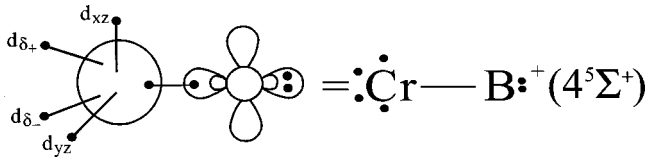


In the $15\,^5\Sigma^+$ state the bonding is comprised of two half $\pi$-bonds and one half $\sigma$-bond. In particular, from the distributions $4s^13d^1_{z^2}3d^{0.50}_{xz}3d^{0.50}_{yz}3d^{1.0}_{x^2-y^2}3d^{1.0}_{xy}$ $(^6D)$, and $2s^{1.89}2p_z^{0.05}2p_x^{0.53}2p_y^{0.53}$ $(^2P)$ of $Cr^+$ and B at infinity, it is obvious that $0.5\,e^-$ are transferred from B to $Cr^+$ through the $\pi$ skeleton forming the two half $\pi$-bonds, while via the $\sigma$-frame a migration of $0.24\,e^-$ occurs from $Cr^+$ to B resulting to two hybrid orbitals $(4s4p_z3d_{z^2})^{1.76}_{Cr^+}/(2s2p_z)^{2.20}_B$ and the formation of a half $\sigma$-bond. The bonding is summarized nicely in the vbL picture,

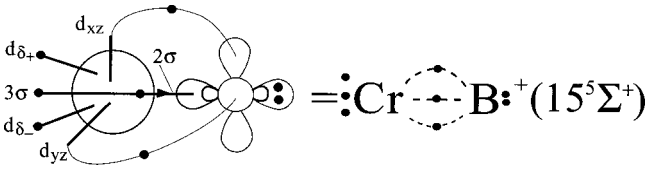


From Table II we read that, at the MRCI level, the 4th and $15\,^5\Sigma^+$ states are characterized by $D_e=33.8$ and 19.4 kcal/mol at $R_e=2.551$ and 2.163 Å, respectively.

### 2. $7\,^5\Delta$, $17\,^5\Delta$

Their origin is traced to the product $|^6D;M=\pm 2,\pm 1\rangle_{Cr^+}\otimes|^2P;M=0,\pm 1\rangle_B$. In both states the asymptotic character of the fragments is maintained along the bonding process. As is evidenced from the leading CASSCF equilibrium CFs as well as from the atomic population analysis,

TABLE III. Total energy $E$ (hartree), bond length $R_e$ (Å), dissociation energy $D_e$ (kcal/mol), and harmonic frequency $\omega_e$ ($cm^{-1}$) of the ground $X\,^7\Sigma^+$ state of $CrB^+$ in different methods.

| Method | $-E$ | $R_e$ | $D_e$ | $\omega_e$ |
|---|---|---|---|---|
| SCF | 1067.698 33 | 2.564 | 19.6 | 248 |
| CISD | 1067.853 29 | 2.350 | 26.5 | 303 |
| CISD+Q[a] | 1067.868 6 | 2.30 | 29 | 326 |
| CASSCF(8/9)[b] | 1067.730 26 | 2.624 | 18.1 | 224 |
| MRCI | 1067.859 63 | 2.335 | 27.0 | 300 |
| MRCI+Q[a] | 1067.868 4 | 2.29 | 29 | 322 |
| sa-CASSCF(8/10)[c,d] | 1067.719 11 | 2.282 | 27.7 | 345 |
| MRCI | 1067.861 64 | 2.265 | 31.3 | 356 |
| MRCI+Q[a] | 1067.872 5 | 2.27 | 32 | 350 |
| CASSCF(8/10)[d] | 1067.740 67 | 2.606 | 18.8 | 257 |
| MRCI | 1067.863 45 | 2.242 | 28.8 | 436 |
| MRCI+Q[a] | 1067.870 5 | 2.23 | 31 | 462 |
| c-MRCI[e] | 1068.146 67 | 2.230 | 30.1 | |
| c-MRCI+Q[a] | 1068.178 5 | 2.20 | 34 | |
| CASSCF(8/10)[d,f] | 1067.741 94 | 2.593 | 18.8 | 271 |
| MRCI | 1067.866 56 | 2.242 | 29.1 | 392 |
| MRCI+Q[a] | 1067.873 7 | 2.23 | 31 | 410 |

[a] $+Q$ refers to the Davidson correction, Ref. 14.
[b] 8/9 means 8 active $e^-$ distributed to 9 orbitals, $(3d)_{Cr}/(2s+2p)_B$.
[c] State average CASSCF.
[d] 8 active $e^-$ distributed to 10 orbitals, $(4s+3d)_{Cr}/(2s+2p)_B$.
[e] The ''core'' $3s^23p^6\,Cr^+\,e^-$ are included in the CI.
[f] The cc-pVQZ basis was employed for the B atom.

$$|7\,^5\Delta\rangle\sim 0.86|1\sigma^22\sigma^23\sigma^11\delta_+^11\pi_x^11\pi_y^1\rangle,$$

$$4s^{1.13}4p_z^{0.08}3d_{z^2}^{1.04}3d_{xz}^{1.0}3d_{yz}^{1.0}3d_{x^2-y^2}^{1.0}/$$
$$2s^{1.89}2p_z^{0.81}2p_x^{0.06}2p_y^{0.06},$$

$$|17\,^5\Delta\rangle\sim 0.44|1\sigma^22\sigma^13\sigma^11\delta_+^1(1\pi_x^2-1\pi_y^2)1\delta_-^1\rangle$$
$$+0.37|1\sigma^22\sigma^13\sigma^11\delta_+^1(1\pi_x^12\bar{\pi}_x^1$$
$$-1\pi_y^12\bar{\pi}_y^1)1\delta_-^1\rangle,$$

$$4s^{0.88}4p_z^{0.08}3d_{z^2}^{1.0}3d_{xz}^{0.60}3d_{yz}^{0.60}3d_{x^2-y^2}^{1.0}3d_{xy}^{1.0}/$$
$$2s^{1.58}2p_z^{0.45}2p_x^{0.40}2p_y^{0.40},$$

the bonding is comprised of a $\sigma$-bond and a $\pi$-bond in the $7\,^5\Delta$ and $17\,^5\Delta$ states, respectively. In the $7\,^5\Delta$ state $4\,e^-$ are fully localized on the $d_\pi$, $d_\sigma$, and $d_{\delta_+}$ (or $d_{\delta_-}$ in the $A_1$ symmetry) orbitals, with $0.20\,e^-$ moving from the B $(2s2p_z)^{2.89}$ hybrid orbital (at infinity) to $Cr^+$ via the $\sigma$ frame. The vbL bonding icon is

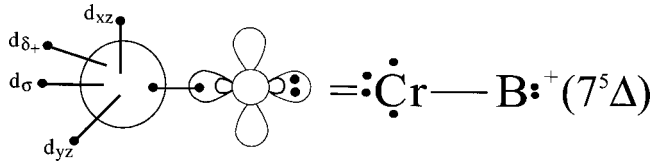


The corresponding bonding icon for the $17\,^5\Delta$ can be drawn as follows:

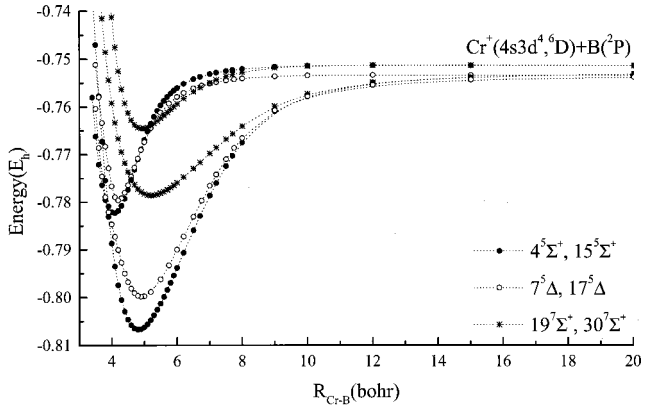


FIG. 4. MRCI PECs of the states $4\,^5\Sigma^+$, $7\,^5\Delta$, $15\,^5\Sigma^+$, $17\,^5\Delta$, $19\,^7\Sigma^+$, and $30\,^7\Sigma^+$.

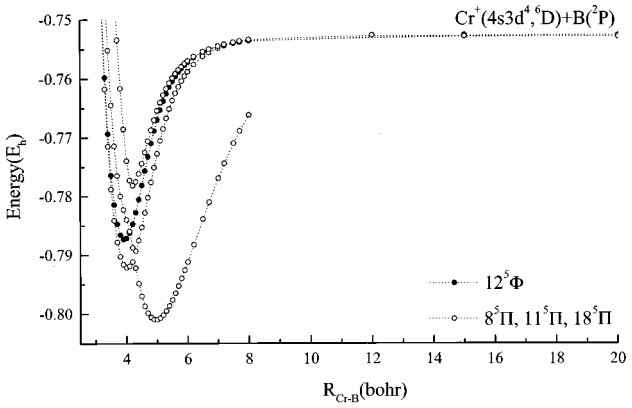


FIG. 5. MRCI PECs of the states $8\,^5\Pi$, $11\,^5\Pi$, $12\,^5\Phi$, and $18\,^5\Pi$.

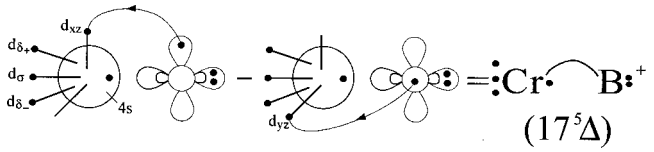


with $0.20\,e^-$ moving along the $\pi$ frame from B to $Cr^+$. The PECs of the above two states are given in Fig. 4; dissociation energies are 29.3 and 16.5 kcal/mol, with corresponding bond distances of 2.611 and 2.231 Å for the 7th and $17\,^5\Delta$ states, respectively.

### 3. $8\,^5\Pi$, $11\,^5\Pi$, $18\,^5\Pi$, $12\,^5\Phi$

The three $^5\Pi$ states correlate to $|^6D;M=\pm1,0,\pm2\rangle_{Cr^+}\otimes|^2P;M=0,\pm1,\mp1\rangle_B$. Their PECs shown in Fig. 5 interact strongly in the inter-atomic region of 4–4.5 bohr. The $8\,^5\Pi$ state, due to an avoided crossing around 4.3 bohr with the $11\,^5\Pi$ state, presents a global ($g$) and a local ($l$) minimum at distances of 2.623 and 2.126 Å, and $D_e=30.6$ and 25.0 kcal/mol, respectively (Table II). The energy barrier measured from the $g$-minimum is 6.3 kcal/mol. At the $g$-minimum the dominant CASSCF configurations,

$$|8\,^5\Pi\rangle\sim0.77|1\sigma^2 2\sigma^2 1\delta_+^1 3\sigma^1 1\pi_y^1 1\delta_-^1\rangle - 0.40|1\sigma^2 2\sigma^1 1\delta_+^1 3\sigma^1 4\bar{\sigma}^1 1\pi_y^1 1\delta_-^1\rangle,$$

coupled with the atomic Mulliken distributions,

$$4s^{1.07}4p_z^{0.07}3d_{z^2}^{1.05}3d_{xz}^{0.04}3d_{yz}^{1.0}3d_{x^2-y^2}^{1.0}3d_{xy}^{1.0}/\;2s^{1.82}2p_z^{0.80}2p_x^{0.09}2p_y^{0.06},$$

indicate the formation of a $\sigma$-bond and four nonbonded (observer) $d_\sigma$, $d_\pi$, and $d_\delta$ electrons,

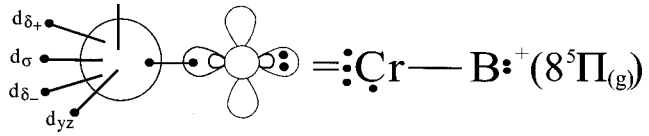


At the $l$-minimum the wave function carries the character of the $11\,^5\Pi$ and $18\,^5\Pi$ states, due to the strong interaction of the latter with the former.

The minimum of the $11\,^5\Pi$ state occurs at 2.27 Å (= 4.3 bohr), the interaction point of the three $\Pi$ states. At this distance its binding energy is 23 kcal/mol but obviously with a very fuzzy binding mode.

The $18\,^5\Pi$ state has a binding energy of 16.2 kcal/mol at $R_e=2.224$ Å and a very unclear binding mode due to its entanglement with the 8th and $11\,^5\Pi$ states.

The $M=\pm2$ and $M=\pm1$ combination of $Cr^+$ and B atoms creates the $12\,^5\Phi$ state whose PEC is also shown in Fig. 5. The main CASSCF CFs, defining in essence the binding scheme, are

$$|12\,^5\Phi\rangle\sim0.56(|1\sigma^2 2\sigma^1 3\sigma^1 1\pi_x^2 1\pi_y^1 1\delta_-^1\rangle - |1\sigma^2 2\sigma^1 1\delta_+^1 3\sigma^1 1\pi_x^1 1\pi_y^2\rangle),$$

leading to a binding picture of a half $\sigma$- and one $\pi$-bond,

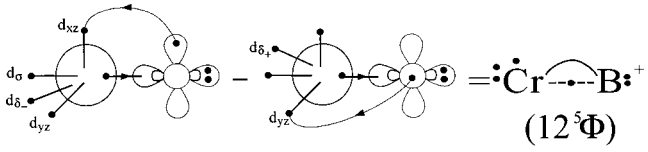


The above icon is corroborated by the Mulliken CASSCF atomic densities,

$$4s^{0.84}4p_z^{0.09}3d_{z^2}^{0.98}3d_{xz}^{1.12}3d_{yz}^{1.12}3d_{x^2-y^2}^{0.52}3d_{xy}^{0.52}/\;2s^{1.53}2p_z^{0.52}2p_x^{0.35}2p_y^{0.35}.$$

A migration of $0.10\,e^-$ is observed from $Cr^+$ to B along the $\sigma$ skeleton resulting in the B hybrid $(2s2p_z)^{2.05}$ orbital, followed by a back donation of $0.30\,e^-$ via the $\pi$ frame. At the MCRCI level Table II records a $D_e=21.6$ kcal/mol at $R_e=2.079$ Å.

### 4. $19\,^7\Sigma^+$, $30\,^7\Sigma^+$

The $19\,^7\Sigma^+$ is very similar to the ground $X\,^7\Sigma^+$ state (*vide supra*), the difference being the replacement of a $3\sigma$ with a $4\sigma$ molecular orbital,

$$|19\,^7\Sigma^+\rangle \sim 0.97|1\sigma^2 2\sigma^1 4\sigma^1 1\delta_+^1 1\pi_x^1 1\pi_y^1 1\delta_-^1\rangle.$$

The CASSCF populations,

$$4s^{0.79}4p_z^{0.17}3d_{z^2}^{0.24}3d_{xz}^{1.0}3d_{yz}^{1.0}3d_{x^2-y^2}^{1.0}3d_{xy}^{1.0}/$$
$$2s^{1.80}2p_z^{0.90}2p_x^{0.05}2p_y^{0.05}$$

indicate the complete localization of the $d_\pi$ and $d_\delta e^-$ on the metal, and the transfer of $0.2\,e^-$ from B to $Cr^+$ along the $\sigma$-route, causing a binding energy of 16.2 kcal/mol at $R_e = 2.757$ Å (Table II, Fig. 4).

The $30\,^7\Sigma^+$ state tracing its lineage to $Cr^+(^6D;M=\pm1)+B(^2P;M=\mp1)$, has a shallow minimum of 8.2 kcal/mol at $R_e = 2.613$ Å (Fig. 4, Table II) with the following CASSCF atomic populations:

$$4s^{0.89}4p_z^{0.09}3d_{z^2}^{1.0}3d_{xz}^{0.58}3d_{yz}^{0.58}3d_{x^2-y^2}^{1.0}3d_{xy}^{1.0}/$$
$$2s^{1.75}2p_z^{0.21}2p_x^{0.44}2p_y^{0.44}.$$

A $(2s2p_z)^{1.96}$ hybridization is observed on the B atom, but with no charge transfer from B to $Cr^+$ through the $\sigma$ skeleton, and a $0.18\,e^-$ transfer from B ($2p_x^{0.53}2p_y^{0.53}$ at infinity) to $Cr^+$ via the $\pi$ system causing a small $\pi$ interaction.

#### 5. $21\,^5\Sigma^-$, $27\,^7\Sigma^-$

Both states correlate to $Cr^+(^6D;M=\pm1)+B(^2P;M=\mp1)$ with their PECs shown in Fig. 6, and with the following leading CASSCF equilibrium CFs:

$$|21\,^5\Sigma^-\rangle \sim 0.41|1\sigma^2 2\sigma^1 3\sigma^1 1\delta_+^1(1\pi_x^2+1\pi_y^2)1\delta_-^1\rangle$$
$$+0.40|1\sigma^2 2\sigma^1 3\sigma^1 1\delta_+^1(1\pi_x^1 2\bar{\pi}_x^1$$
$$+1\pi_y^1 2\bar{\pi}_y^1)1\delta_-^1\rangle,$$
$$|27\,^7\Sigma^-\rangle \sim 0.69|1\sigma^2 2\sigma^1 3\sigma^1 1\delta_+^1(1\pi_x^1 2\pi_x^1$$
$$+1\pi_y^1 2\pi_y^1)1\delta_-^1\rangle.$$

In the $21\,^5\Sigma^-$ state we have the development of a weak $\pi$-bond giving rise to a $D_e = 12.3$ kcal/mol at $R_e = 2.203$ Å, while in the $27\,^7\Sigma^-$ state the two atoms interact weakly in a rather electrostatic fashion resulting in a $D_e = 8.2$ kcal/mol at $R_e = 2.453$ Å.

#### 6. $22\,^7\Pi$, $26\,^7\Pi$, $29\,^7\Pi$, $24\,^7\Phi$

The following product wave functions describe the $\Pi$ and $\Phi$ states asymptotically:

$$|22\,^7\Pi,26\,^7\Pi,29\,^7\Pi,24\,^7\Phi\rangle = |^6D;M=\pm1,0,\pm2,$$
$$\pm2\rangle_{Cr^+}\otimes|^2P;M=0,\pm1,$$
$$\mp1,\pm1\rangle_B.$$

The PECs shown in Fig. 7 indicate low dissociation energies, and also the interwoven nature of the $\Pi$ states due to avoided crossings resulting in an interchange of the character of their (global) minima. In particular, the equilibrium of the $22\,^7\Pi$ and $26\,^7\Pi$ states carry the asymptotic character of the 26th and $29\,^7\Pi$ states, respectively. The complete localization of the four $3d\,e^-$ on the $Cr^+$ in conjunction with the high spin do not allow for any strong binding: the $D_e$'s of the 22, 26, $29\,^7\Pi$, and $24\,^7\Phi$ states are 13.0, 9.3, 7.3, and 9.9 kcal/mol at 2.381, 2.393, 2.65, and 2.367 Å, respectively (Table II). Only in the $22\,^7\Pi$ state there is a $0.20\,e^-$ transfer from B to $Cr^+$ via the $\sigma$-frame and perhaps the development of a half $\sigma$-bond; in the rest of the states the charge transfer is insignificant.

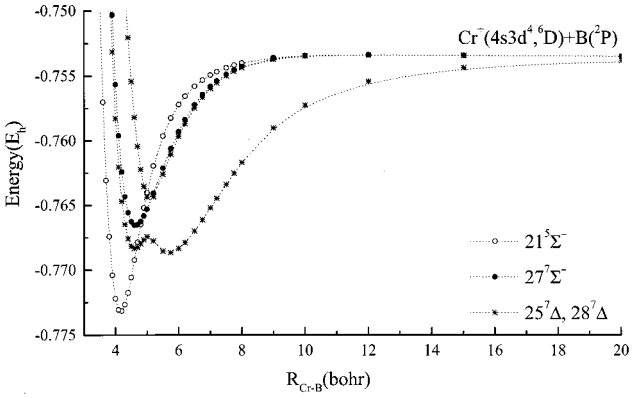


FIG. 6. MRCI PECs of the states $21\,^5\Sigma^-$, $25\,^7\Delta$, $27\,^7\Sigma^-$, and $28\,^7\Delta$.

#### 7. $25\,^7\Delta$, $28\,^7\Delta$

Figure 6 presents the PECs of the titled states correlating to $|^6D;M=\pm2,\pm1\rangle_{Cr^+}\otimes|^2P;M=0,\pm1\rangle_B$. The $25\,^7\Delta$ suffers an avoided crossing at about 5 bohr with the incoming $28\,^7\Delta$ state resulting in two, practically degenerate, minima at the MRCI level, Table II. Again, the high spin and the $d$ localization of the $Cr^+$ electrons forbid any significant binding. The asymptotic electron distributions are essentially transferred to the first minimum of the $25\,^7\Delta$ state ($R_e = 3.015$ Å), while as expected, the minimum of the $28\,^7\Delta$ state being on top of the barrier, is a mélange of the two asymptotes, $0.57|M=\pm2\rangle\otimes|M=0\rangle+0.53|M=\pm1\rangle\otimes|M=\pm1\rangle$. From Table II we read that the $D_e$'s and $R_e$'s are 9.5, 7.1 kcal/mol and 3.015, 2.710 Å for the 25 and $28\,^7\Delta$ states, respectively.

### C. $5\,^3\Delta$, $6\,^3\Pi$, $9\,^3\Sigma^-$, $10\,^3\Phi$, $13\,^3\Pi$, $14\,^3\Delta$, $16\,^3\Sigma^+$, $23\,^3\Pi$, and $33\,^3\Sigma^+$ states

All the above triplet states correlate to $Cr^+(4s3d^4,\,^4D)+B(2s^22p,\,^2P)$.

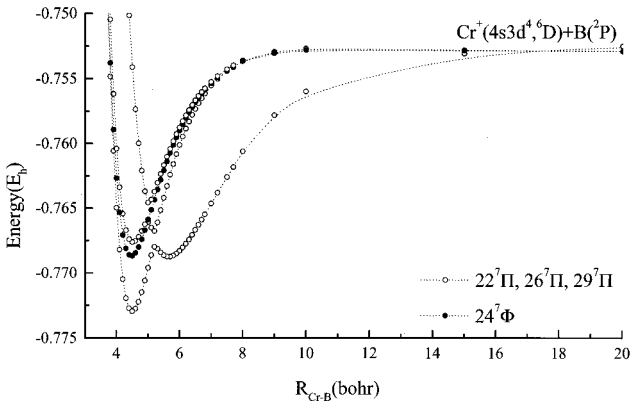


FIG. 7. MRCI PECs of the states $22\,^7\Pi$, $24\,^7\Phi$, $26\,^7\Pi$, and $29\,^7\Pi$.

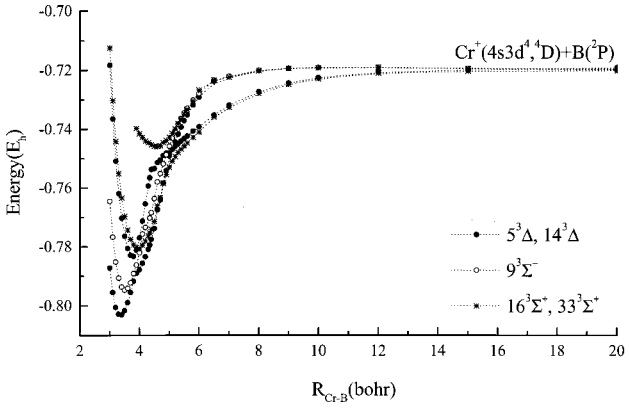


FIG. 8. MRCI PECs of the states $5\,^3\Delta$, $9\,^3\Sigma^-$, $14\,^3\Delta$, $16\,^3\Sigma^+$, and $33\,^3\Sigma^+$.

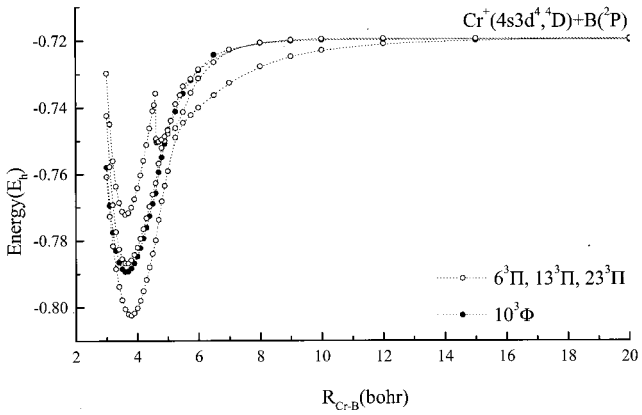


FIG. 9. MRCI PECs of the states $6\,^3\Pi$, $10\,^3\Phi$, $13\,^3\Pi$, and $23\,^3\Pi$.

### 1. $5\,^3\Delta$, $14\,^3\Delta$

The adiabatic fragments of the Δ states are described by the combination $|^4D;M=\pm 2,\pm 1\rangle_{Cr^+}\otimes|^2P;M=0,\pm 1\rangle_B$ with MRCI PECs given in Fig. 8. Around 5 bohr a character change of the $5\,^3\Delta$ state is observed ($M=\pm 2,0$ to $\pm 1$, $\pm 1$) due to an avoided crossing with the $14\,^3\Delta$ state; a second avoided crossing follows at about 4 bohr responsible for the equilibrium personality of this state, i.e., that of a triple bond (*vide infra*). The leading CASSCF configurations are

$$|5\,^3\Delta\rangle \sim 0.85|1\sigma^2 2\sigma^1 1\delta_+^1 1\pi_x^2 1\pi_y^2\rangle - 0.16|1\sigma^2 2\sigma^1 1\delta_+^1 1\pi_x^2 2\pi_y^2\rangle - 0.16|1\sigma^2 2\sigma^1 1\delta_+^1 2\pi_x^2 1\pi_y^2\rangle,$$

with the ''0.16'' components signifying the GVB correlation. The CASSCF atomic Mulliken populations,

$$4s^{0.28}4p_z^{0.12}3d_{z^2}^{0.91}3d_{xz}^{1.36}3d_{yz}^{1.36}3d_{x^2-y^2}^{1.0}3d_{xy}^{0.07}/ 2s^{1.47}2p_z^{0.25}2p_x^{0.55}2p_y^{0.55},$$

reveal the existence of a triple bond, in accord with the ''0.85'' CASSCF component. We can draw the following vbL picture:

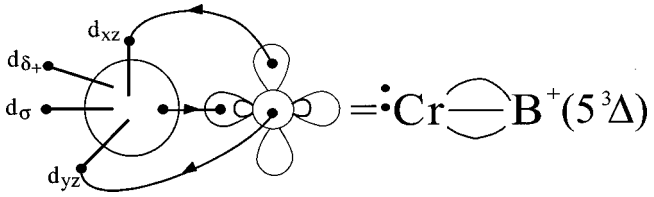


Notice that the *in situ* B atom finds itself in a $^4P$ excited state, 3.57 eV above the ground $^2P$ state (Table I). Therefore, through the $\pi$ frame $2\times 0.36=0.72\,e^-$ are transferred from the B to the metal center, with the latter responding back with $0.6\,e^-$ via the $\sigma$-frame. Our binding energy of 52.9 kcal/mol, with respect to the adiabatic fragments, and bond length of 1.779 Å (Table II), are in remarkable agreement with the isovalent species $CrCH^+$ $(\tilde{X}\,^3\Sigma^-)^{15(a)}$ and $CrN^+$ $(X^3\Sigma^-)^{15(b)}$ with corresponding parameters of 53.7 kcal/mol, 1.772 Å and 49.5 kcal/mol, 1.569 Å, respectively. Certainly, all three species have very similar electron distributions, the only difference being the occupation of a $\delta_-$ orbital ($CrB^+$) instead of a $d_\sigma$ orbital ($CrCH^+$,$CrN^+$). Finally, we report that the $5\,^3\Delta$ state has the shortest bond length of all states studied (Table II), with an ''internal bond strength'' of $52.9+\Delta E(^4P\leftarrow{}^2P)=135$ kcal/mol, in harmony with its triple bond character.

The $14\,^3\Delta$ suffers three avoided crossings, two of which (the first and the third) at 5.0 and 4.0 bohr have been previously discussed, and another one between the first two (~4.3 bohr) and an incoming $^3\Delta$ state (not calculated) originating from the $^4P$ boron state and responsible for the triple bond character in both the 5th and $14\,^3\Delta$ states. Due to the fact that the $14\,^3\Delta$ minimum occurs at the interaction region with the $5\,^3\Delta$ state, it carries the memory of both states. Our main equilibrium CASSCF configurations are

$$|14\,^3\Delta\rangle \sim 0.53|1\sigma^2 2\sigma^1 1\delta_+^1 1\pi_x^2 1\pi_y^2\rangle + 0.37|1\sigma^2 2\sigma^2 1\delta_+^1(1\bar{\pi}_x^1 1\pi_y^1 - 1\pi_x^1 1\bar{\pi}_y^1)1\delta_-^1\rangle.$$

Clearly, the ''0.53'' component introduces the triple bond character, while the ''0.37'' correlates to the $M=\pm 1,\pm 1$ asymptote. At $R_e=1.985$ Å a $D_e=39.9$ kcal/mol is calculated at the MRCI level, Table II.

### 2. $6\,^3\Pi$, $13\,^3\Pi$, $23\,^3\Pi$, $10\,^3\Phi$

At infinity the 6th, 13th, $23\,^3\Pi$, and $10\,^3\Phi$ states correlate to $|^4D;M=\pm 1,\pm 2,0,\pm 2\rangle_{Cr^+}\otimes|^2P;M=0,\mp 1,\pm 1,\pm 1\rangle_B$, respectively, with corresponding PECs shown in Fig. 9. The involved morphology of the Π symmetry curves is caused by consecutive avoided crossings discussed briefly in what follows.

At large distance (~6 bohr) a strong interaction between the 13th and $23\,^3\Pi$ states changes their character ($M=\pm 2$, $\mp 1\rightarrow 0,\pm 1$), followed by an avoided crossing at 5.3 bohr between the 6th and the $13\,^3\Pi$ states, resulting to the character transfer of the latter to the former. The net result is the adoption of the $23\,^3\Pi$ character ($M=0,\pm 1$) by the $6\,^3\Pi$ state. Another avoided crossing occurs between the 13th and the $23\,^3\Pi$ states, thus the 13th re-enters into its former asymptotic mode. Now, the $23\,^3\Pi$ state experiences a severe

avoided crossing at about 4.5 bohr with an incoming (not calculated) $^3\Pi$ state stemming from the $Cr^+$ $^4G$ atomic state.

At the equilibrium the predominant parent configuration of the $6\,^3\Pi$ state is of the type $1\sigma^2(2\sigma^1 1\delta_+^1 1\pi_x^2 1\pi_y^1 1\delta_-^1)$ combined with a series of spin functions coupled into a triplet. Apart from the formation of a $\pi$ bond, the localization of two $\delta e^-$ on the metal, and a net transfer of $0.1\,e^-$ from B to $Cr^+$ nothing else can be said about the bonding nature of the $6\,^3\Pi$ state. From Table II we read that a $D_e = 52.3$ kcal/mol is obtained at $R_e = 2.003$ Å (MRCI).

The dominant CASSCF equilibrium configurations of the $13\,^3\Pi$ and $23\,^3\Pi$ states are

$$|13^3\Pi\rangle \sim 0.39(|1\sigma^2 2\sigma^2 1\delta_+^1 1\pi_x^1 1\pi_y^2\rangle - |1\sigma^2 2\sigma^2 1\pi_x^2 1\pi_y^1 1\delta_-^1\rangle) + 0.37|1\sigma^2 2\sigma^1 1\delta_+^1 1\pi_x^2 1\bar{\pi}_y^1 1\delta_-^1\rangle - 0.36|1\sigma^2 2\bar{\sigma}^1 1\delta_+^1 1\pi_x^2 1\pi_y^1 1\delta_-^1\rangle,$$

$$|23^3\Pi\rangle \sim 0.55|1\sigma^2 2\sigma^1 1\delta_+^1 1\pi_x^2 1\bar{\pi}_y^1 1\delta_-^1\rangle - 0.31(|1\sigma^2 2\sigma^1 1\bar{\delta}_+^1 1\pi_x^2 1\pi_y^1 1\delta_-^1\rangle + |1\sigma^2 2\sigma^1 1\delta_+^1 1\pi_x^2 1\pi_y^1 1\bar{\delta}_-^1\rangle).$$

In the $13\,^3\Pi$ state the ''0.39'' and ''0.37, 0.36'' contributions correlate to the $M = (\pm 2, \mp 1)$ and $(0, \pm 1)$ components, respectively, while in the $23\,^3\Pi$ state both ''0.55'' and ''0.31'' configurations correspond to the $M = 0, \pm 1$ adiabatic fragments. The nature of the configurations involved in the above states and the rather unclear populations obtained from the CASSCF wave functions, forbid the construction of simple bonding images. The binding energies and bond distances at the MRCI level (Table II) of the 13th and $23\,^3\Pi$ states are 42.1 and 33.0 kcal/mol, at 1.931 and 1.911 Å, respectively.

The dominant CASSCF equilibrium CFs of the $10\,^3\Phi$ state along with the Mulliken atomic populations are

$$|10^3\Phi\rangle \sim 0.53(|1\sigma^2 2\sigma^2 1\pi_x^2 1\pi_y^1 1\delta_-^1\rangle + |1\sigma^2 2\sigma^2 1\delta_+^1 1\pi_x^1 1\pi_y^2\rangle),$$

$$4s^{0.39}4p_z^{0.15}3d_{z^2}^{1.26}3d_{xz}^{1.12}3d_{yz}^{1.12}3d_{x^2-y^2}^{0.54}3d_{xy}^{0.54}/ 2s^{1.45}2p_z^{0.70}2p_x^{0.34}2p_y^{0.34}.$$

Taking into account the populations at infinity,

$$4s^{1.0}3d_{z^2}^{1.0}3d_{xz}^{1.0}3d_{yz}^{1.0}3d_{x^2-y^2}^{0.50}3d_{xy}^{0.50}/ 2s^{1.89}2p_z^{0.06}2p_x^{0.53}2p_y^{0.53},$$

the following vbL icon can be drawn:

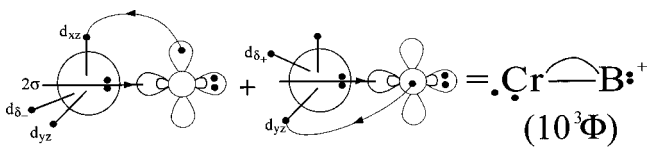


We claim that three $\pi$ electrons are involved in a single $\pi$ bond, while a $\sigma$ bond is formed through the interaction of the hybrid orbital functions $(4s4p_z3d_{z^2})_{Cr^+}^{1.80} + (2s2p_z)_B^{2.15}$, with a net transfer of $0.14\,e^-$ from B to $Cr^+$.

### 3. $9\,^3\Sigma^-$

The present state, described at infinity by the wave function $|^4D; M = \pm 1\rangle_{Cr^+} \otimes |^2P; M = \mp 1\rangle_B$, exhibits an avoided crossing at the internuclear distance of 4.0 bohr with the $20\,^3\Sigma^-$ state (partially computed) which correlates to the $Cr^+$ $^4G$ atomic state (*vide infra*), Fig. 8. The equilibrium CASSCF CFs and the atomic population densities of the $9\,^3\Sigma^-$ state are

$$|9\,^3\Sigma^-\rangle \sim 0.78|1\sigma^2 1\delta_+^1 1\pi_x^2 1\pi_y^2 1\delta_-^1\rangle,$$

$$4s^{0.18}4p_z^{0.10}3d_{z^2}^{0.29}3d_{xz}^{1.26}3d_{yz}^{1.26}3d_{x^2-y^2}^{1.0}3d_{xy}^{1.0}/ 2s^{1.43}2p_z^{0.08}2p_x^{0.66}2p_y^{0.66}.$$

A vbL bonding picture consistent with the above data is the following:

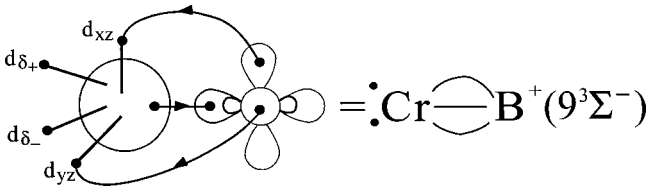


Notice that the *in situ* B atom finds itself in the $^4P$ $(2s^1 2p_x^1 2p_y^1; M = 0)$ excited state. Via the $\pi$-frame $0.52(= 0.26 + 0.26)\,e^-$ are moving from the B to the $Cr^+$ cation forming two $\pi$-bonds; through the $\sigma$-frame $0.43\,e^-$ migrate from a $(4s4p_z3d_{z^2})_{Cr^+}$ hybrid to the $2s(1.43\,e^-)$ of the B atom. The energy content of this triple bond with respect to the adiabatic products is $D_e = 47.3$ kcal/mol at $R_e = 1.864$ Å (Table II).

### 4. $16\,^3\Sigma^+$, $33\,^3\Sigma^+$

The PECs shown in Fig. 8 correlate to $|^4D; M = 0, \pm 1\rangle_{Cr^+} \otimes |^2P; M = 0, \mp 1\rangle_B$, respectively. The equilibrium CASSCF CFs are of the type

$$|16\,^3\Sigma^+\rangle \sim 1\sigma^2 2\sigma^2(1\delta_+^1 1\pi_x^1 1\pi_y^1 1\delta_-^1)$$

and

$$|33^3\Sigma^+\rangle \sim 1\sigma^2(2\sigma^1 3\sigma^1 1\delta_+^1 1\pi_x^1 1\pi_y^1 1\delta_-^1),$$

combined with a series of triplet coupled spin functions. The corresponding Mulliken atomic distributions are

$$16\,^3\Sigma^+: 4s^{0.49}4p_z^{0.15}3d_{z^2}^{1.12}3d_{xz}^{0.66}3d_{yz}^{0.66}3d_{x^2-y^2}^{1.0}3d_{xy}^{1.0}/ 2s^{1.44}2p_z^{0.76}2p_x^{0.34}2p_y^{0.34},$$

$$33\,^3\Sigma^+: 4s^{0.90}4p_z^{0.12}3d_{z^2}^{0.50}3d_{xz}^{0.86}3d_{yz}^{0.86}3d_{x^2-y^2}^{1.0}3d_{xy}^{1.0}/ 2s^{1.62}2p_z^{0.80}2p_x^{0.16}2p_y^{0.16}.$$

The bonding mechanism of the $16\,^3\Sigma^+$ state is succinctly represented by the icon

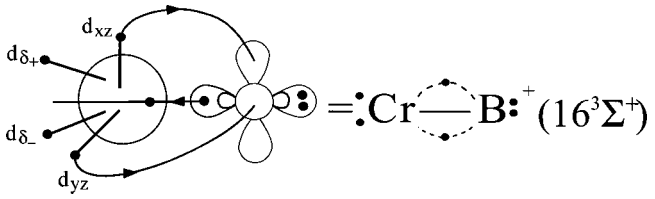


indicating the formation of a $\sigma$-bond and two half $\pi$-bonds. Via the $\pi$-frame $2\times0.34=0.68\,e^-$ diffuse from $Cr^+$ to B, while $0.8\,e^-$ return to the $(4s4p_z3d_{z^2})^{1.76}_{Cr^+}$ hybrid. At a $R_e=2.090$ Å the bond energy content is $D_e=38.0$ kcal/mol with respect to the asymptotic products (Table II).

The bonding in the $33\,^3\Sigma^+$ state is not so clear as in the previous state; we can discern two half $\pi$-bonds with a synchronous transfer of $0.32\,e^-$ through the $\pi$ system, two observer $\delta_+$ and $\delta_-$ $e^-$, and the donation of $0.50\,e^-$ from B to $Cr^+$ via the $\sigma$-frame. At the equilibrium distance of $R_e=2.423$ Å a rather weak bond of 16.5 kcal/mol is calculated at the MRCI level.

### D. $20\,^3\Sigma^-$, $31\,^3\Phi$, $32\,^3\Gamma$, and $34^3\Delta$ states

The four titled states correlate adiabatically to $Cr^+(^4G)+B(^2P)$; no complete potential energy curves are available for these states due to severe technical problems encountered during their computations (Fig. 10).

#### 1. $20^3\Sigma^-$

As was already discussed in Sec. IV C the $20\,^3\Sigma^-$ state suffers an avoided crossing at about 4 bohr with the $9\,^3\Sigma^-$ state (*vide supra*). The fact that the interaction between these two PECs practically coincides with the equilibrium distance of the state under discussion, does not allow for an understanding of the binding in terms of simple ''chemical pictures.'' With respect to the adiabatic products we report a binding energy $D_e=73.0$ kcal/mol at a $R_e=2.075$ Å (Table II).

For the $31\,^3\Phi$ state we can only report its binding energy $D_e=62.5$ kcal/mol and bond length $R_e=1.888$ Å at the MRCI level of theory, Table II.

#### 2. $32^3\Gamma$

This state traces its ancestry to $|^4G;M=\pm4\rangle_{Cr^+}\otimes|^2P;M=0\rangle_B$. The leading CASSCF equilibrium configurations ($A_2$ symmetry) and corresponding Mulliken densities are

$$|32\,^3\Gamma\rangle\sim0.60(|1\sigma^22\sigma^21\pi_x^11\pi_y^11\delta_-^2\rangle - |1\sigma^22\sigma^21\delta_+^21\pi_x^11\pi_y^1\rangle),$$

$$4s^{0.30}4p_z^{0.12}3d_{z^2}^{1.22}3d_{xz}^{0.73}3d_{yz}^{0.73}3d_{x^2-y^2}^{1.0}3d_{xy}^{1.0}/$$

$$2s^{1.55}2p_z^{0.76}2p_x^{0.27}2p_y^{0.27}.$$

We clearly see the formation of two half $\pi$-bonds with the synchronous transfer of $2\times0.27=0.54\,e^-$ from $Cr^+$ to B through the $\pi$ system, and one $\sigma$-bond between the two hybrids $(4s4p_z3d_{z^2})^{1.64}_{Cr^+}$ and $(2s2p_z)^{2.31}_B$. The emerging vbL icon is the following:

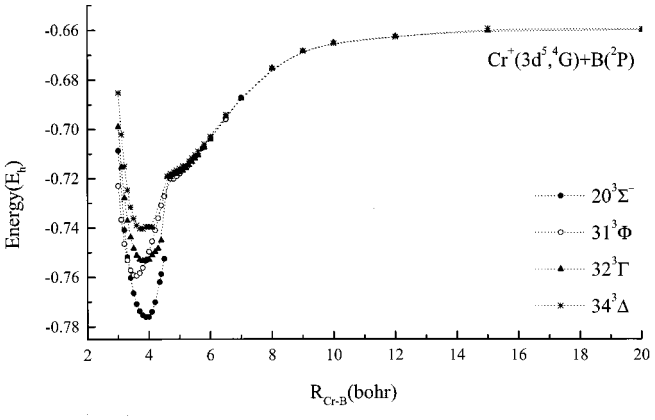


FIG. 10. MRCI PECs of the states $20\,^3\Sigma^-$, $31\,^3\Phi$, $32\,^3\Gamma$, and $34\,^3\Delta$.

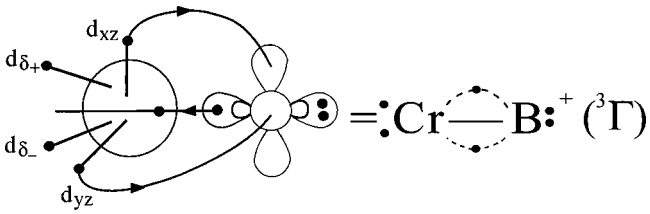


At the MRCI level the dissociation energy and bond distance are 58.7 kcal/mol and 2.020 Å (Table II).

#### 3. $34^3\Delta$

This is the highest state reported in the present work, 3.35 eV above the ground $X\,^7\Sigma^+$ state. The main CASSCF equilibrium CFs,

$$|34\,^3\Delta\rangle\sim0.68|1\sigma^21\delta_+^13\sigma^11\pi_x^21\pi_y^2\rangle - 0.23|1\sigma^22\sigma^11\delta_+^11\pi_x^21\pi_y^2\rangle$$

in conjunction with the Mulliken CASSCF densities,

$$4s^{0.53}4p_z^{0.13}3d_{z^2}^{0.52}3d_{xz}^{1.41}3d_{yz}^{1.41}3d_{x^2-y^2}^{1.0}3d_{xy}^{0.13}/$$

$$2s^{1.36}2p_z^{0.55}2p_x^{0.45}2p_y^{0.45},$$

dictate the formation of a triple bond; as expected the *in situ* B atom is in its excited $^4P$ state. Although the $3d_{xy}$ $0.13\,e^-$ cannot be accounted for, it is rather clear that about $1\,e^-$ is transferred from B to $Cr^+$ via the $\pi$ frame and the formation of two $\pi$-bonds, while $0.9\,e^-$ are injected back from the metal to the B atom through the $\sigma$-frame. As we can see from Table II the binding energy $D_e=50.5$ kcal/mol at an $R_e=1.986$ Å, is very similar to the other triple bonded states $5\,^3\Delta$ and $9\,^3\Sigma^-$.

## V. SYNOPSIS AND FINAL REMARKS

Employing a $[(7s6p4d3f)_{Cr}/(4s3p2d1f)_B]$ basis in conjunction with CASSCF-CI methods, we have investigated the electronic structure of the molecular cation chromium boride, $CrB^+$.

For the ground $(X\,^7\Sigma^+)$ and thirty four excited states we report MRCI potential curves, absolute energies, and spectroscopic constants $(R_e, D_e, \omega_e, T_e)$. We also tried to inter-

pret the binding interactions by the use of simple chemical diagrams. Our main findings can be condensed as follows:

Given that the *in situ* B atom is in its lowest state, the $X\,^7\Sigma^+$ state of $CrB^+$ has the maximal spin multiplicity possible, is rather loosely bound ($D_e = 28.8$ kcal/mol), and the two atoms are held together by a half $\sigma$-bond. The complete lack of $\pi$ interaction stemming from $Cr^+$ is interpreted on the basis of the significantly larger ionization potential of $Cr^+$ as compared to the earlier transition metal cations. It is reminded that the ground states of the previous borides studied, i.e., $ScB^+(X\,^4\Sigma^-)$, $TiB^+(X\,^5\Delta)$, $VB^+(X\,^6\Sigma^+)$ have a mean binding energy of 45 kcal/mol, while the bonding is comprised of three half-bonds, one $\sigma$, and two $\pi$.

We have encountered a variety of binding schemes ranging from a half $\sigma$ to full three bonds, and bond distances from 2.76($19\,^7\Sigma^+$) to 1.78($5\,^3\Delta$) Å.

The state $5\,^3\Delta$, $9\,^3\Sigma^-$, and $34\,^3\Delta$ present genuinely three bond character with binding energies of 52.9, 47.3, and 50.5 kcal/mol, respectively.

It is obvious that within the accuracy of our methods the high density of a number of states, for instance the $5\,^3\Delta$, $6\,^3\Pi$, $7\,^5\Delta$, and $8\,^5\Pi$ with energy differences less than 1 mhartree, preclude the accurate determination of their relative energy ordering.

Drawing on our previous experience, some numerical experiments done in the present report and the indicative results of the Davidson correction, we can claim that on the average, our MRCI $D_e$ values fall short by about 7% as compared to the ''true'' $D_e$ numbers.

Finally, with the exception of the four first states $X\,^7\Sigma^+$, $1\,^5\Sigma^+$, $2\,^5\Pi$ and $3\,^7\Pi$ all states are unbound with respect to the ground state atoms.


[1] (a) A. Kalemos and A. Mavridis, Adv. Quantum Chem. **32**, 69 (1998); (b) A. Kalemos and A. Mavridis, J. Phys. Chem. A **102**, 5982 (1998); (c) A. Kalemos and A. Mavridis, *ibid.* **103**, 3336 (1999).

[2] C. E. Moore, *Atomic Energy Levels*, NSRDS-NBS Circular 3 (U.S. Government Printing Office, Washington, DC, 1971).

[3] C. W. Bauschlicher, Jr., Theor. Chim. Acta **92**, 183 (1995).

[4] T. H. Dunning, Jr., J. Chem. Phys. **90**, 1007 (1989).

[5] H.-J. Werner and P. J. Knowles, J. Chem. Phys. **89**, 5803 (1988); P. J. Knowles, and H.-J. Werner, Chem. Phys. Lett. **145**, 514 (1988); H.-J. Werner and E. A. Reinsch, J. Chem. Phys. **76**, 3144 (1982); H.-J. Werner, Adv. Chem. Phys. **LXIX**, 1 (1987).

[6] M. Couty and M. B. Hall, J. Phys. Chem. A **101**, 6936 (1997).

[7] A. I. Krylov, D. C. Sherill, E. F. C. Byrd, and M. Head-Gordon, J. Chem. Phys. **109**, 10669 (1998).

[8] R. J. Bartlett, Annu. Rev. Phys. Chem. **32**, 359 (1981).

[9] W. Duch and G. H. F. Diercksen, J. Chem. Phys. **101**, 3018 (1994).

[10] K. Docken and J. Hinze, J. Chem. Phys. **57**, 4928 (1972); H.-J. Werner and W. Meyer, *ibid.* **74**, 5794 (1981).

[11] MOLPRO is a package of *ab initio* programs written by H.-J. Werner and P. J. Knowles, with contributions from J. Almlöf *et al.*

[12] H. Partridge, J. Chem. Phys. **90**, 1043 (1989).

[13] T. Koga, H. Tatewaki, and A. J. Thakkar, J. Chem. Phys. **100**, 8140 (1994).

[14] S. R. Langhoff and E. R. Davidson, Int. J. Quantum Chem. **8**, 61 (1974); M. R. A. Blomberg and P. E. M. Siegbahn, J. Chem. Phys. **78**, 5682 (1983).

[15] (a) A. Mavridis, A. E. Alvarado-Swaisgood, and J. F. Harrison, J. Phys. Chem. **90**, 2584 (1986); (b) K. L. Kunze and J. F. Harrison, *ibid.* **93**, 2983 (1989).